



## Review of 2 kW grid connected LOPF tests in Nissum Bredning

Margheritini, Lucia

*Publication date:*  
2017

*Document Version*  
Publisher's PDF, also known as Version of record

[Link to publication from Aalborg University](#)

*Citation for published version (APA):*

Margheritini, L. (2017). *Review of 2 kW grid connected LOPF tests in Nissum Bredning*. Department of Civil Engineering, Aalborg University. DCE Technical reports No. 231

### General rights

Copyright and moral rights for the publications made accessible in the public portal are retained by the authors and/or other copyright owners and it is a condition of accessing publications that users recognise and abide by the legal requirements associated with these rights.

- Users may download and print one copy of any publication from the public portal for the purpose of private study or research.
- You may not further distribute the material or use it for any profit-making activity or commercial gain
- You may freely distribute the URL identifying the publication in the public portal -

### Take down policy

If you believe that this document breaches copyright please contact us at [vbn@aub.aau.dk](mailto:vbn@aub.aau.dk) providing details, and we will remove access to the work immediately and investigate your claim.



**DEPARTMENT OF CIVIL ENGINEERING**  
AALBORG UNIVERSITY

# **Review of 2 kW grid connected LOPF tests in Nissum Bredning**

**Lucia Margheritini**



Title

Aalborg University  
Department of Civil Engineering  
Group Name

**DCE Technical Report No. 231**

# **Review of 2 kW grid connected LOPF tests in Nissum Bredning**

by

Lucia Margheritini

July 2017

© Aalborg University

Published 2017 by  
Aalborg University  
Department of Civil Engineering  
Sofiendalsvej 9-11  
DK-9200 Aalborg SV, Denmark

Printed in Aalborg at Aalborg University

ISSN 1901-726X  
DCE Technical Report No. 231

## Contents

1. Introduction.....	6
2. Objectives .....	7
3. Setup: Main buoy elements and measuring system .....	8
3.1 The buoy .....	8
3.2 Wave measurements .....	10
3.3 Calibration of sensors .....	13
4. Results from the testing campaign .....	14
4.1 Analysis of results and consideration .....	15
5. Compliance with the target power curve in the 10787 project. ....	18
6. Conclusions.....	20
Appendix A.....	21
Appendix B.....	24
APPENDIX C – Future improvements.....	29

# 1. Introduction

This report has been prepared by Per Resen and Aalborg University for the ForskVE project 10878: **2 kW grid connected LOPF test buoy**.

AAU has the role of reviewing and advise on the data analysis, besides compiling this report.

The purpose of this project was to document the mechanical power production against a target power curve of a 2kW grid connected wave energy buoy in Nissum Bredning at Helligsø. This test site is typically used for open sea testing of scale 1:10 devices in irregular waves. In order to better adapt to the moderate wave height, the buoy was down sized by a factor of 3 and a new lower target power curve for the buoy was agreed to. Downsizing the project also had the advantage that it is more cost effective and fast to experiment with small wave energy devices than with big devices, at an early development stage, in line with the TRL and four phases development (proof of concept, design and feasibility study, field trials and half or full-scale trials) promoted by AAU and supported by the marine renewable energy sector. To complement this, the IEC 114 standards define 3 stages of testing (1=small scale and no scaled version of PTO, 2=PTO represents a realistic full-scale PTO with adjustable control strategies, 3=realistic PTO function and full-scale machine with all electrical component working as they should).

With this project LOPF classifies somewhere in stage 1-2 of the IEC 114 and stage 2-3 of the AAU four stages of development.

A ForskVE project has an element of design work as well as documenting the actual power production of a grid connected device in the sea. The granted funds available are partly dependent on the success of meeting or exceeding the agreed target power curve. For wave energy devices, it is agreed that the mechanical power is measured as a reference vs significant wave height.

This document contains a concise introduction in Ch.1, a list of objectives of the investigations in Ch.2 and a description of the WEC and the set up in Ch. 3. Ch. 4 presents the results from the tests and an analysis including time series of the average Mechanical Power during the testing period in Summer 2017 (total of 700 hours) and its relation to wave conditions; efficiency in different wave conditions, time series of torque vs wave height. Ch. 5 present the compliance with the power curve set as a target by the ForskVE project 10878. Finally, Ch.6 includes the conclusions. Appendix A, B, C include wave analysis, cut off frequencies, future work and instrument details respectively.

## 2. Objectives

The objectives of this project are:

- To design and construction of the test buoy with a 10 Hz data logging capability.
- To operate the grid connected buoy in the sea.
- To document and measure the mechanical power production vs significant wave height over a minimum period of 600 hours, equivalent to 25 days, against the agreed target power production.



### 3. Setup: Main buoy elements and measuring system

In this chapter, the main buoy elements and the measuring equipment will be described.

#### 3.1 The buoy

The buoy consists of the float (that provides the buoyancy and stability) and the drum, that revolves around a center axis (mounted to the float on both sides) and which contains the mechanical components and power take off of the device (Fig. 1). A mooring line is wrapped around the drum in a rubber belt, on the drum, and the other end of the mooring line is attached to the sea bed. When a wave passes it pushes respectively the buoy forth and back and up down within each wave action and makes the drum rotate forth and back (pivoting on the axis connected to the float) and activates the generator inside the drum.

The main shaft on the drum is connected to the generator inside the drum, through 2 specific gearboxes, one to accelerate the angular speed and the second to make the generator shaft rotate in only one direction. Inside the drum there is also a spring (which position is regulated by a small electrical motor) that connects the main shaft to the drum and which performs two functions:

- 1) It brings back the rotational drum to its original position after each wave stroke.
- 2) It regulates the pre-tensioning of the drum to the sea bed and also the draught of the buoy, optimizing the power production for any sea condition.

The pre-tensioning mechanism also allows for full submersion of the buoy during storms to protect the buoy against un controlled loads.

For measuring the absorbed mechanical power on the main shaft, two different sensors are used:

- Absolute encoder, which measures the absolute angular position between the main shaft and the drum, and from which the angular speed can be calculated.
- Strain gauges on the main shaft measures the torque acting on the main shaft.

The absorbed mechanical power into the power take off system is calculated as the torque on the main shaft multiplied by the angular speed of the drum.

The small scale devise can be seen in position at the test location in Fig. 2

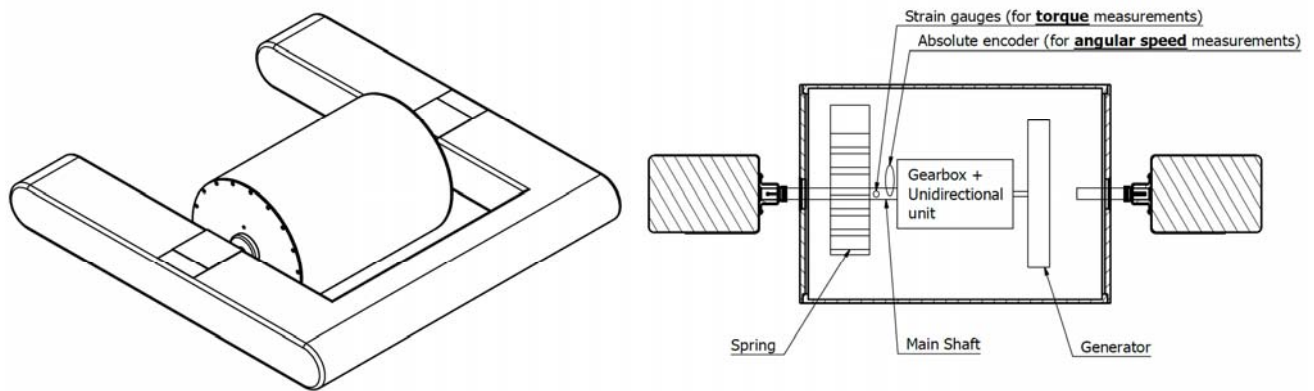


Figure 1. Drawing of LOPF and internal PTO and monitoring equipment

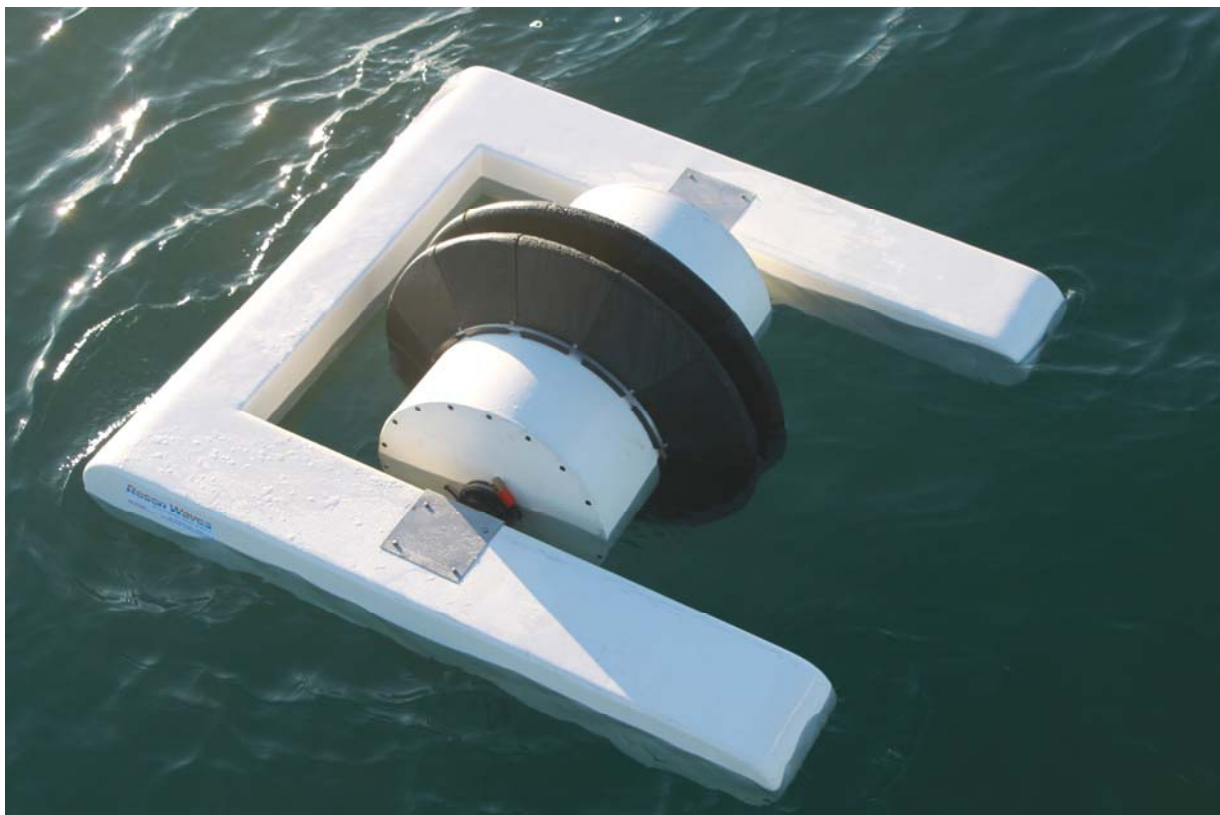


Figure 2. LOPF sea trial Nissum Bredning. Stage 3 of AAU development.

Below Fig.3&4, an example is shown of what the data looks like for both sensors when logged at 10 Hz in an irregular sea-state.

The product of the two variables at any time provide the value of the mechanical power absorbed, which is then averaged in 15 minutes intervals /time slots.

During the same time, the significant wave height is also calculated to represents the average sea-state as significant wave height  $H_s$ . When logged at 10 Hz it produces 9.000 readings in 15 minutes intervals.

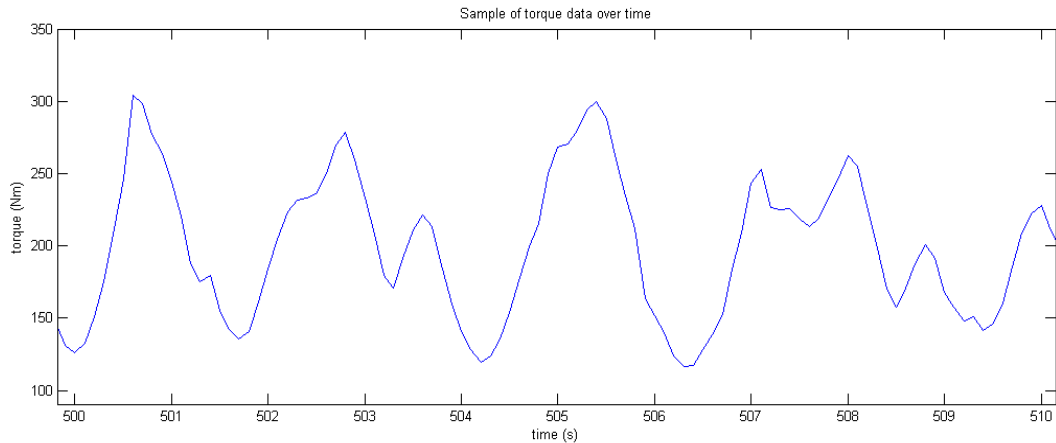


Figure 3. Typical torque measurements from torque transducer over 4 wave periods.

The torque varies with the wave stroke, because the spring coefficient (stiffness) is steep vs. the turning angle of the spring inside the drum. An ideal spring coefficient is fairly flat and does not vary much with the turning of the drum. The pre-tensioning of the buoy represents the average torque, which is adjusted for tidal variation to maintain a desired average torque and also controls the powerproduction.

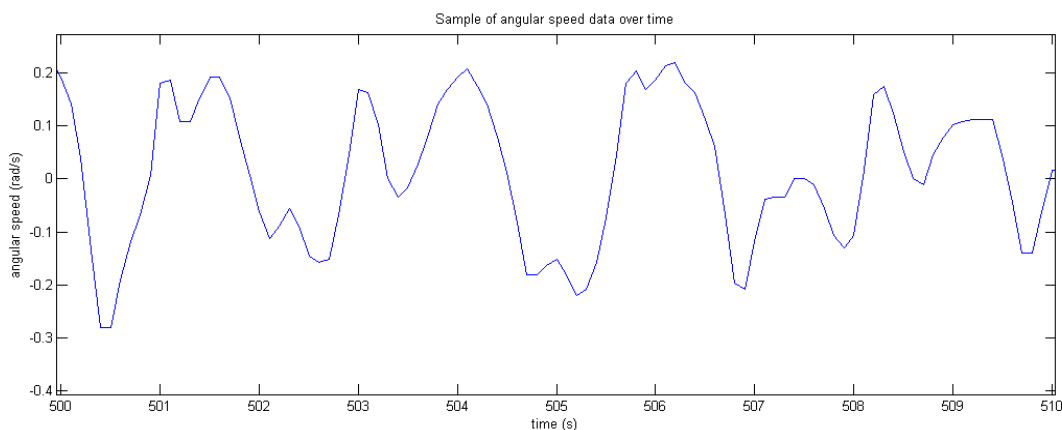


Figure 4. Typical angular speed calculated from absolute encoder over 4 wave periods.

### 3.2 Wave measurements

Wave elevations are measured through the use of a pressure sensor installed at the end of a pole on a small dock, as shown in Fig. 5&6.

The pressure sensor is positioned approximately  $\frac{1}{2}$  m below the water surface at low tide in an area with a typical tidal variation of  $\pm \frac{1}{2}$  m. During storms, there is a storm surge of  $1\frac{1}{2}$  m. The normal water depth is 3,5 m.

The pressure sensor is placed 6 m from the wave buoy and on the on side towards the typical wave front.



*Figure 5. Pressure sensor is on the pole on the right side of the ladder.*

The pressure sensor (Fig. 5) provides a time series of the water pressure above the sensor. The back side of the pressure diaphragm is vented towards the atmospheric pressure, which cancels out the variation in atmospheric pressure. Through correction and analysis in the frequency domain with a cut off frequency of 0,8 Hz, it is possible to calculate the surface elevation and the main wave parameters like significant wave height, wave period and wave power per m wave front, at any sea state.

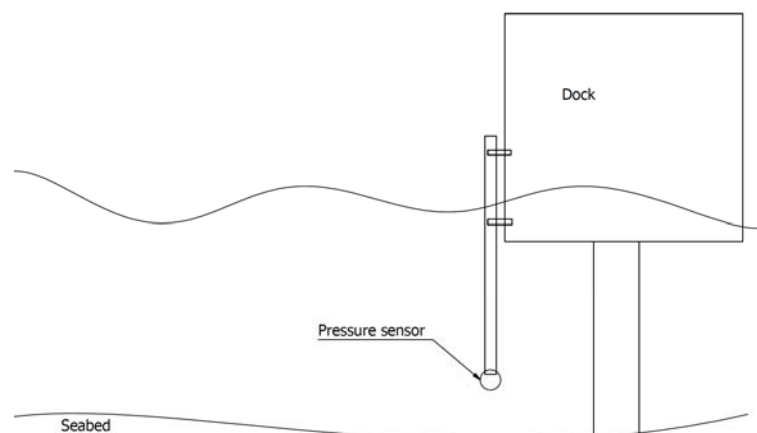


*Figure 6. Schematics of Picture in Fig. 5*

In Fig.7 is shown an example of what the data looks like for wave measurements (before and after the pressure density function has been applied). It is a 10 second recording in a random sea-state, before and after processing of the data. The high cut off frequency on the pressure sensor is 0,8 Hz:

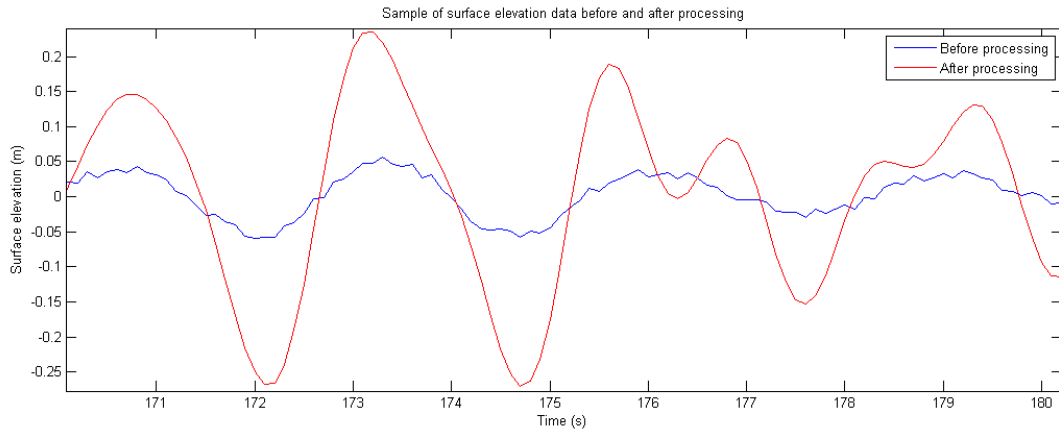


Figure 7. Typical analyzed data of surface elevations

As a side note, the measurements in the buoy and the measurements from the pressure sensor are not directly relatable at the same position, since it is not possible to exactly measure the waves where the device is, because the device interferes with the waves if the pressure sensor is too close to the device. In this setup, the distance is 6 m between the device and the pressure sensor. But by averaging all data over 15 min. time slots the distance of 6 m is averaged out and is not a source of error. In Fig. 8 the wave heights and period distribution during the testing period are presented.

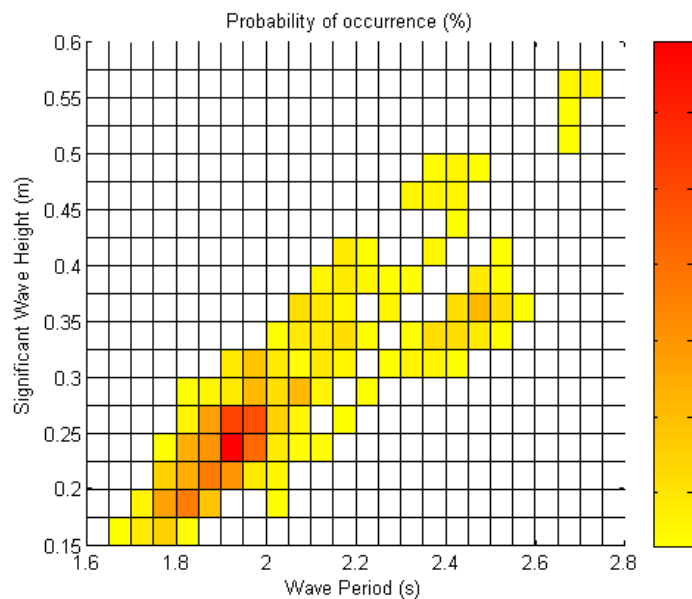


Figure 8. Wave height and period distributions.

### 3.3 Calibration of sensors

The torque on the main shaft has been calibrated by applying several weights of respectively 1, 5, 6, 13, 20 and 40 kg on a 1m arm applying torques from zero and up to 400 Nm. The unfiltered measurements are very stable with a very low noise level below 0,3 Nm.

Strain gauge full bridge on the main drive shaft into the drive system. RW design.

The angular measurements with 12-bit resolution (4.096 per revolution) was checked for any scaling errors. SICK absolute encoder.

The pressure sensor was calibrated at an accredited test center to provide 4 to 20 mA outputs from 0 to 10m water column, and compensated for atmospheric pressure. HJ-Jensen PDS-10 adapted for continuous sea operation.

More details in wave data analysis and processing of the power data can be found in the Appendixes.



## 4. Results from the testing campaign

Once the measurements for each sea state in 15-minute time slots have been processed and the average quantities of torque (X) angular speed = mechanical power,  $H_s$  significant wave height, wave period and the power per m wave front, respectively have been calculated for each sea-state  $H_s$ , it is possible to have a look at the general behavior of the buoy.

Based on the 15-minute average the mechanical power vs the incoming wave power (assuming a physical capture width equal to the width of the float, which is 60 cm) looks like Fig. 9:

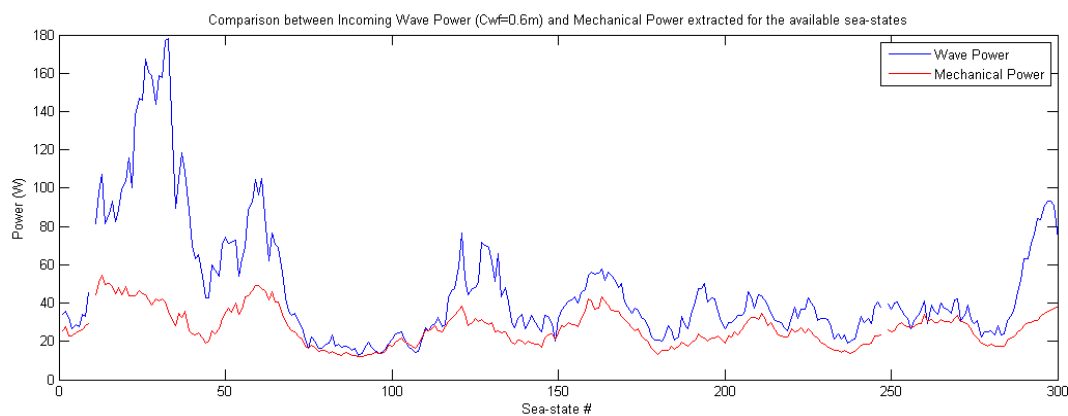


Figure 9. Mechanical power plotted with incoming wave power over 75 hours and 300 time slots of 15 min.

It shows good correlation between incoming and absorbed power respectively, something special for the buoy, because the rotational movement of the drum is directly converted to electric power with direct drive and direct wave action with a pre-tensioned buoy.

It can also be seen, that for high seas (higher power) only a small portion of the available power is being used. That is due to the effect of the current spring, which has a steep spring characteristic. The use of springs with a flatter spring stiffness in the future, will dramatically improve the power production in bigger waves, as shown in APPENDIX C.

The efficiency at different sea-states  $H_s$  is shown below. It can be observed that the efficiency is around 100% in small waves and drops off in higher  $H_s$ , due the steep spring characteristics.

With a flat spring characteristic it is expected the high efficiency of 100% also will apply for bigger waves.

Max efficiencies (>70%) were achieved for wave heights between 0.15 and 0.25 m and periods between 1.6 and 2.2 s, which were also the most probable waves at location, Fig. 10.

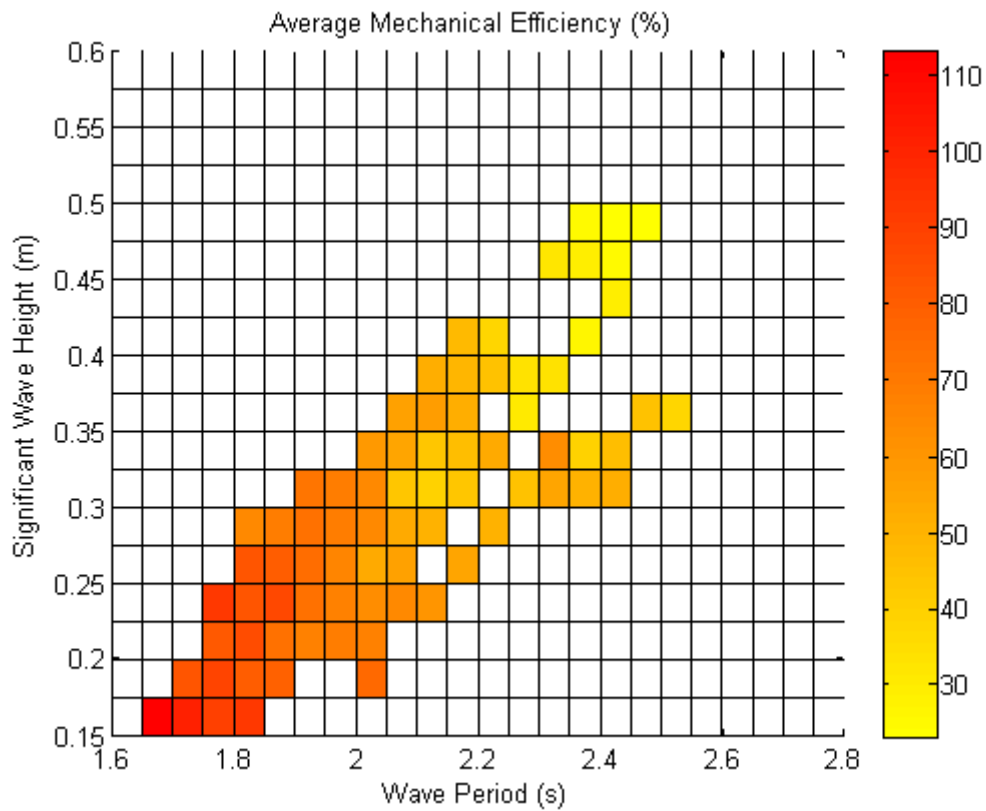


Figure 10. Average mechanical power in different wave conditions during the testing period.

## 4.1 Analysis of results and consideration

Once the data is organized into sea-states in 15-minute time slots it is interesting to look at trends and patterns. That is done by sorting the data against one specific parameter.

Below it is shown the correlation between the power absorbed and the significant wave height. The blue line is a poly fit line in the data. Each dot represents a 15-minute average (Fig 11).

In Fig. 12 we can see the wave period influence of the absorbed mechanical power, for the same wave height.



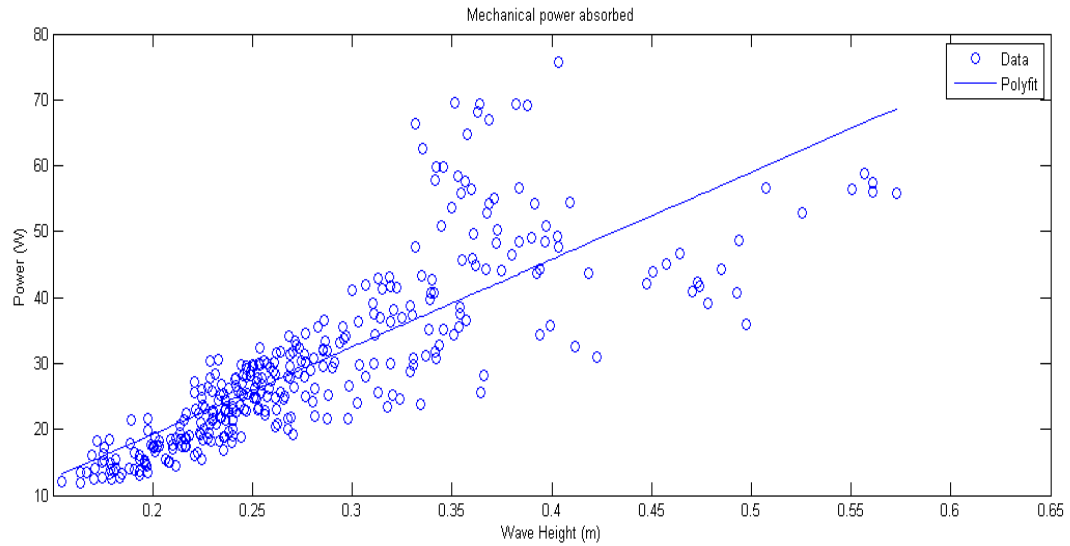


Figure 11. Mechanical Power vs wave height

Alternatively, we can also show how efficient the buoy is at different wave heights, plotting the capture width, which is defined as the ratio between mechanical power and incoming wave power.

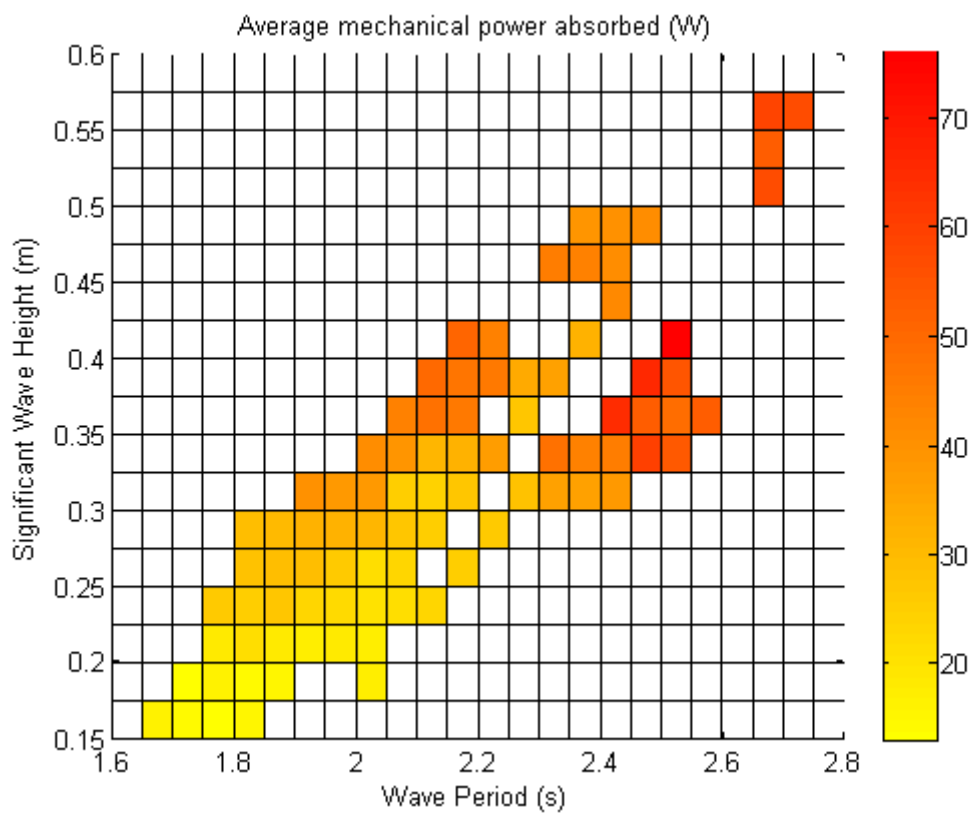


Figure 12. Average mechanical power in different wave conditions during testing period.

It is observed there is a strong correlation between torque and wave height and wave height and rotational speed, Fig. 13 and 14.

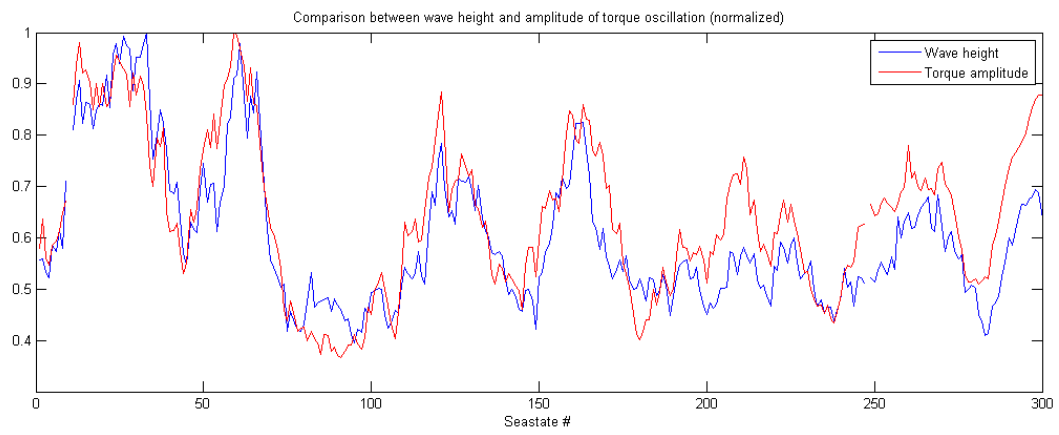


Figure 13. Sample from time series of wave height and Torque measurements.

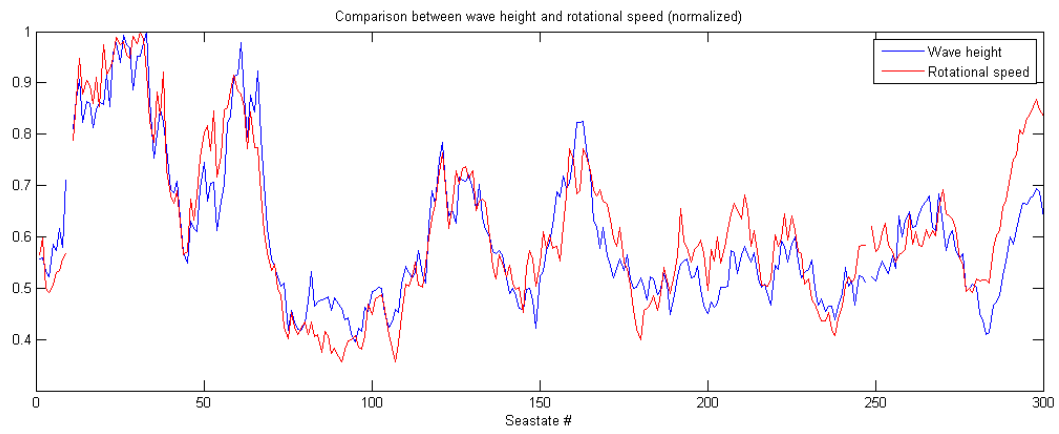


Figure 14. Sample from time series of wave height and rotational speed measurement.

## 5. Compliance with the target power curve in the 10787 project.

In this chapter the obtained data will be plotted against the target curve and it will be demonstrated how they exceed the expected performance.

The performance of the buoy against the agreed target power curve is presented both in table 1 and Fig. 15:

Table 1. Target curve by average wave height  $H_m$

$H_m$ : [cm]	Average mechanical power W, 15 min intervals	EI
<7	n.a.	
From 7 to 13	$P_{mek} = 0,9 + ((H_m - 7) * 0,617) \text{ W}$	Wh =
From 13 to 20	$P_{mek} = 4,6 + ((H_m - 13) * 1,09) \text{ W}$	Wh =
From 20 to 27	$P_{mek} = 12,2 + ((H_m - 20) * 1,33) \text{ W}$	Wh =
From 27 to 33	$P_{mek} = 21,5 + ((H_m - 27) * 1,62) \text{ W}$	Wh =
Greater than 33	$P_{mek} = 31,2 \text{ W}$	Wh =

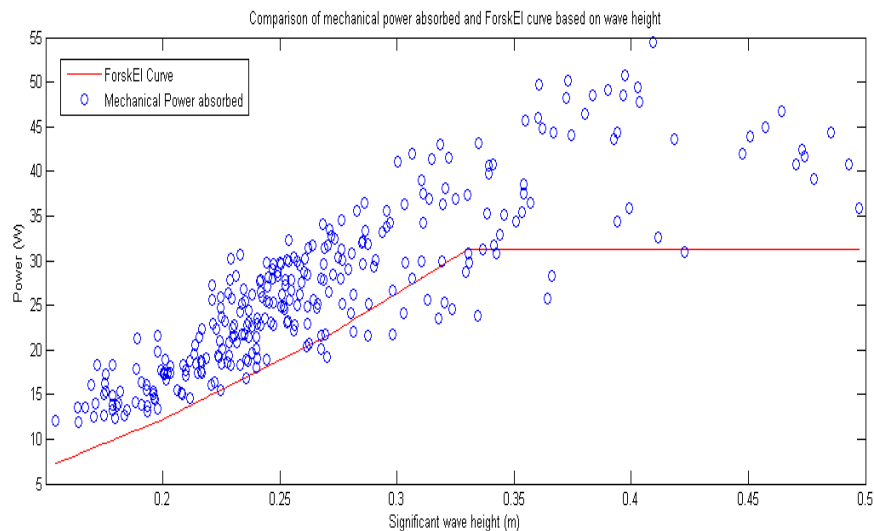


Figure 15. Target curve in the form Power (W), (top) vs wave height and measured performance (bottom).

The power figures during the measuring campaign are shown against the reference target power curve as it can be seen in Fig.15. For the majority of the data point, the LOPF exceeded the expected performance by 90% in average. Each blue dot represents the results for the mechanical power absorbed during one sea state (15 minutes). In this example 335 valid results out of 343 are above the red target power curve, which is 91% above target, which is typical for the measurement.

Each dot represents a 15-minute average power production and average significant wave height against the red, target power curve.

## 6. Conclusions

- Design and construction of the LOPF buoy with data acquisition system and PTO have been achieved successfully. These achievements and the realization of the tests classify the LOPF at stage 2-3 in the AAU phases of development and 1-2 in the IEC 114 standards for the Marine Energy sector.
- The buoy until now operated for 720 hours equivalent to 30 days in the relevant sea environment.
- The mechanical power vs the significant wave height has been monitored and documented against the target power curve for a period of 720 hours of which it has been on or over performing the target curve for 649 hours. The requirement for the ForskVE contract was minimum 600 hours.
- The buoy will continue the operation in the sea for another 3 to 6 months.
- The min. and max. mechanical power measured here are 20 and 70 W respectively across wave height from 0.15 to 0.60 m. Max. efficiencies (>70%) were achieved for wave heights between 0.15 and 0.25 m and periods between 1.6 and 2.2 s, which were also the most probable waves at location recorded during the testing period. This result is promising in terms of having a full scale device ranging on MW scale.
- The buoy concept shows remarkable high (80-100%) efficiency in picking up the wave power in small waves from 3 cm Hs. This is interesting and should be investigated further in more energetic seas.

## Appendix A

### From pressure readings to surface elevation, Wave Spectrum and power in 26-01-2016

#### Logs to relative pressure

In each data file, data is recorded in voltage, being 4.27 V the atmospheric pressure and 20.32 V 10 times the atmospheric pressure (10 meters below water level) for pressure sensor #159979. Removing the atmospheric pressure from the equation, the relative pressure will be:

$$p_{rel} = (V - 4.27) * \frac{10 * 101325}{(20.32 - 4.27)} \text{ Pa}$$

#### Relative pressure to surface elevation

The relative pressure is indicator of the water column above the pressure sensor, which depends on the depth  $z$  at which the water depth is installed and the surface elevation  $\eta$ , which is the height (positive or negative) of the water from the mean water level. That variates over time and it's due to the waves. At any moment:

$$p_{rel}(t) = -\rho g z + \rho g K_p \eta(t)$$

Where:

$$-\rho g z = p_{mean}$$

And  $K_p$  is a corrector factor for waves. Since  $K_p$  depends also on the frequency of the waves will be looked later on, after the wave spectrum has been computed.

We can now rewrite the equation as:

$$\eta = \frac{p'}{\rho g K_p}, \quad \text{where } p' = p_{rel} - p_{mean}$$

#### Surface elevation to Wave Spectrum

At this point, after having converted the readings into surface elevation, it is possible to generate the energy spectrum for each individual sea state. To do that, it is needed to do a FFT (Fourier Fast Transform), to understand how much energy each interval of frequency brings to the sea state.

Through the FFT we can theorize that any irregular sea state is composed by the sum of many different waves, each with its own amplitude, frequency and phase. The surface elevation can be then rewritten as:

$$\eta(t) = a_0 + \sum_{n=1}^{\infty} [a_n \cos(n\omega t) + b_n \sin(n\omega t)]$$

$\omega$  indicates the basic angular frequency increment that we are using for the FFT. To bring it back to actual frequency  $\omega = 2\pi f$ .

$a_0$ ,  $a_n$  and  $b_n$  can be then calculated as:

$$a_0 = \frac{1}{T} \int_0^T \eta(t) dt, \quad a_n = \frac{2}{T} \int_0^T \eta(t) \cos(n\omega t) dt, \quad b_n = \frac{2}{T} \int_0^T \eta(t) \sin(n\omega t) dt$$

Since:

$$a_n \cos(n\omega t) + b_n \sin(n\omega t) = A_n \cos(n\omega t - \beta_n)$$

We can rewrite:

$$A_n = \sqrt{a_n^2 + b_n^2} \quad , \quad \beta_n = \tan^{-1}\left(\frac{b_n}{a_n}\right)$$

And finally the surface elevation can be rewritten as:

$$\eta(t) = A_0 + \sum_{n=1}^{\infty} A_n \cos(n\omega t - \beta_n)$$

Lastly, before generating the spectrum, we limit the frequency value at high frequency, since waves with frequency higher than 0.5/1 Hz are due to noise or just wrinkles. Setting then  $N_c \Leftrightarrow f=1\text{Hz}$ :

$$\eta(t) = A_0 + \sum_{n=1}^{N_c} A_n \cos(n\omega t - \beta_n)$$

Finally, the amplitude spectrum can be calculated as:

$$S(\omega) = \frac{1}{2} A(\omega)^2$$

With  $n$  going from 1 to  $N_c$ .

### **Introduction of pressure transfer function $K_p$**

The pressure transfer function  $K_p$  is defined as:

$$K_p(z, h, \omega) = \frac{\cosh(k(h + z))}{\cosh(kh)}$$

Where  $h$  is the water depth (that changes over time due to tide),  $z$  is the distance between the sensor and the free surface (previously calculated) and  $\omega$  is the angular frequency.

At a certain point total water depth has been measured as  $h=2.85$  and distance from the probe and the surface as  $z=1.42\text{m}$  and therefore  $h=z+1.43\text{m}$  we can rewrite the equation as:

$$K_p(z, \omega) = \frac{\cosh(k(z + 1.43 + z))}{\cosh(k(z + 1.43))}$$

Knowing that:

$$k = \frac{2\pi}{L} \quad \text{and} \quad L = \frac{gT^2}{2\pi} \tanh \frac{2\pi h}{L}$$

We can now calculate  $K_p$  for any combination of depth (every 5 cm between 3 m and 6 m) and frequency.

As a note, due to the fact that the calculation of  $L$  takes quite some time (as it is made through many iterations), I pre-calculated all the values of  $K_p$  for any combination of frequency and water depth, so that while analyzing the data we just need to look which was the depth when each data file was recorded.

Once  $K_p$  is calculated, the surface elevation can be rewritten as:

$$\eta(t) = A_0 + \sum_{n=1}^{N_c} \frac{A_n}{K_p} \cos(n\omega t - \beta_n)$$

And the amplitude spectrum as:

$$S(\omega) = \frac{1}{2} \frac{A(\omega)^2}{K_p(\omega)^2}$$

The surface elevation is then plotted before and after the introduction of  $K_p$  for a visual verification of the process (after introducing  $K_p$ , waves should be shown higher than before).

### **Power Calculation**

Power available in a sea state can be calculated in different ways.

The first method used to evaluate the power available in the area is through the use of the energy period ( $T_e$ ), and significant wave height ( $H_{m0}$ ) represented by the formula:

$$P_e = \frac{\rho g^2}{64\pi} H_{m0}^2 T_e$$

$T_e$  and  $H_{m0}$  were both obtainable from the analysis of the spectrum, through the formulas

$$H_{m0} = 4.004 \sqrt{m_0} \quad , \quad T_{m01} = \frac{m_0}{m_1}$$

Being  $m_0$  and  $m_1$ , obtainable from the relation:

$$m_n = \int_0^\infty f^n S(f) df$$

Or, as before, assuming that we are using the cut out frequency  $f_c=1$  Hz:

$$m_n = \int_0^{N_c} f^n S(f) df$$

And calculable with the sum of the various components (same as for the energy spectrum), multiplied these times for the correspondent power of the frequencies values such as in the example below:

$$m_{-1} = \sum_0^{N_c} f^{-1} * S(f) * \Delta f$$

Alternatively the energy period can also be calculated as:

$$T_e = \frac{m_{-1}}{m_0} \quad or \quad T_{m02} = \sqrt{\frac{m_0}{m_2}}$$

Another way to calculate the power available is to integrate the spectrum over the frequency, multiplying the contribution of each interval of frequency by its own group celerity, as shown below:

$$P = \rho g \int_0^{N_c} S(f) * C_g(f) df$$

Where

$$C_g(\omega, h) = \frac{1}{2} C_p \left( 1 + \frac{2kh}{\sinh(2kh)} \right)$$

And

$$C_p = \left( \frac{g}{k} \tanh(kh) \right)^{1/2} \quad , \quad k = \frac{2\pi}{L}$$

Same as before for  $Kp$ , all the values of  $C_g$  (that depends on frequency and water depth) have been pre-calculated and the values for the actual water depth in any data logging, is retrieved by the program.

Power will then be calculated in both ways to have more reliable results for the sea state.

### **Validation and time domain analysis**

Once the pressure data has been converted in surface elevation (and after the introduction of  $Kp$ ) the data can be also used for the analysis in the time domain. That has the main function of validation, checking that all the parameters calculated in the frequency domain are valid.

$H_{1/3}$  and  $T_{1/3}$  are calculated as the height and period of the highest third of the waves in the time sequence. That has been done using the zero up-crossing method and using a filter to not count waves smaller than 1 second (as they would be just wrinkles).



## Appendix B

### Selection of appropriate Cut-Off Frequency (COF) 12-04-2017

#### Pressure transfer function

The pressure transfer function  $K_p$  represents the correction to the amplitude of different frequencies waves that needs to be taken into account when performing converting pressure reading into surface elevation.

In fact, the movement of the water particles generated by any frequency is attenuated over the height of the water column, meaning that their movement reduces while going deeper into the water column. Hence the need of a correction factor to be applied to the measurements for the pressure sensor.  $K_p$  is defined as:

$$K_p(z, h, \omega) = \frac{\cosh(k(h + z))}{\cosh(kh)}$$

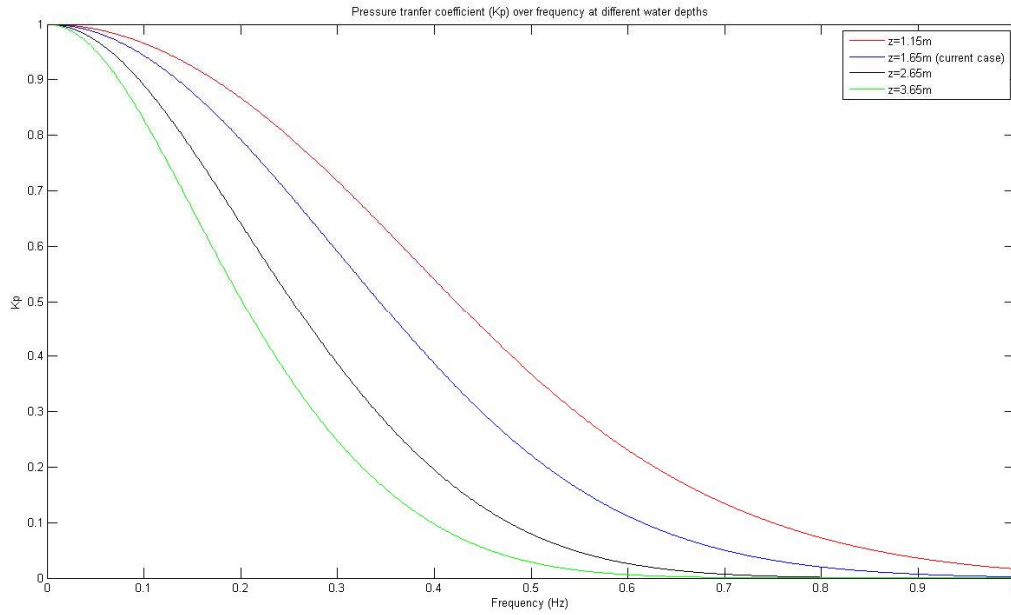
Where  $h$  is the water depth (that changes over time due to tide),  $z$  is the distance between the sensor and the free surface (previously calculated) and  $\omega$  is the angular frequency, over which  $k$  depends/ In this specific case we know that the pressure sensor is located 1.43 m over the seabed and therefore we can rewrite the equation as:

$$K_p(z, \omega) = \frac{\cosh(k(z + 1.43 + z))}{\cosh(k(z + 1.43))}$$

After calculating the values of  $K_p$  for different water depths and any frequency between 0.001 and 1 Hz, it is easy to notice that the coefficient tends to 0 for higher frequencies. That is logical, since the effect of very ‘fast’ waves (meaning high frequency) will be harder to collect as the waves would be smaller and their particles movement would attenuate very rapidly over the water column.

Secondly, it can be noticed that the higher is the distance between the sensor and the water surface, the higher the coefficient tends to 0. That also makes sense since the there is more ‘space’ for the particles movement to reduce.

Both effects are shown in the graph below, which presents the  $K_p$  coefficient over the frequency, for different water depths, where the blue line is the case used for the calculation that will follow.



In reality, when  $K_p$  tends to 0 it represents the fact that the pressure sensor is basically unable to receive any data from those high frequencies, hence the very small value of  $K_p$ . However, since the correction happens through the formula:

$$\eta(t) = A_0 + \sum_{n=1}^{N_c} \frac{A_n}{K_p} \cos(n\omega t - \beta_n)$$

We would be introducing a very high uncertainty as, dividing any amplitude by a value of  $K_p$  as small as  $10^{-4}$  it would increase dramatically any error in the amplitude value calculated from the pressure sensor data.

### **Process**

The process of the analysis can be divided into two separate parts:

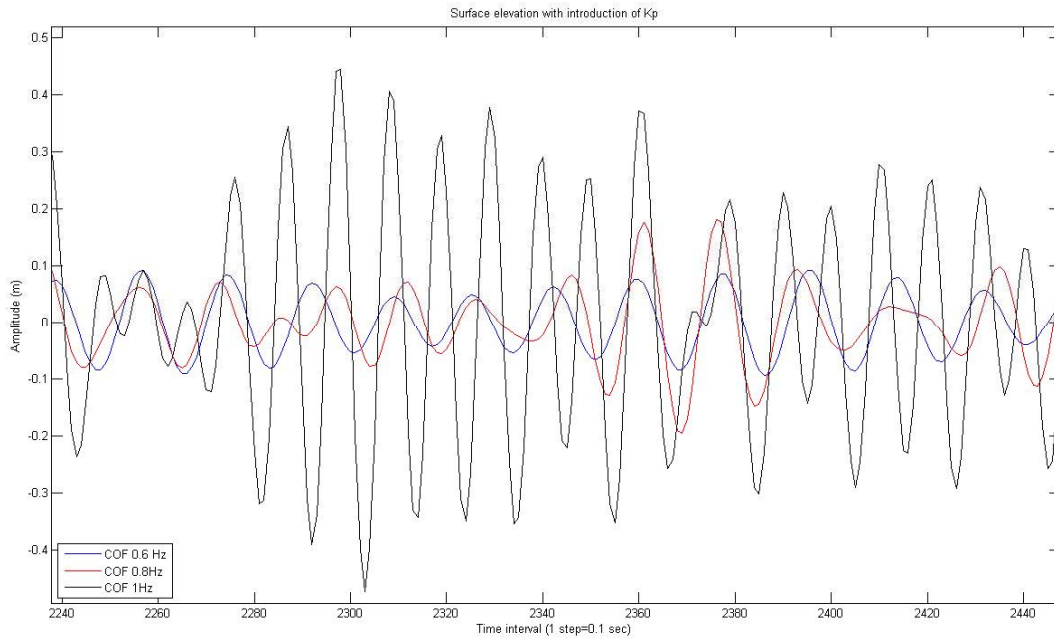
- The selection of the relevant data through the use of the COF applied to the process of the FFT.
- The introduction of the pressure transfer function.

For logical continuity with the general discussion of this report we will look first in the second part of the process and then into the first part.

### **Effects of $K_p$ on processed data depending on the selected COF**

The effect of the introduction  $K_p$  depending on the selected COF is shown below, where it is plotted a portion of a seastate (case 2 in the rovided raw data file). For this particular case, we were able physically see the sea state at the test site and we could see that waves were high maximum around 20 cm.

Below it is shown the effect of using different COF (0.6 Hz, 0.8Hz, 1Hz) on the calculated surface elevation after the introduction of  $K_p$ .



It can be easily seen that while for COF of 0.6 and 0.8 Hz the values remain around the expected value (around 20cm wave height), while the black line (COF 1 Hz) shows much higher waves, up to almost 1 m. That is due to the impact of the extremely low value of  $K_p$  of the higher frequencies.

### **Selection of relevant data depending on selected COF**

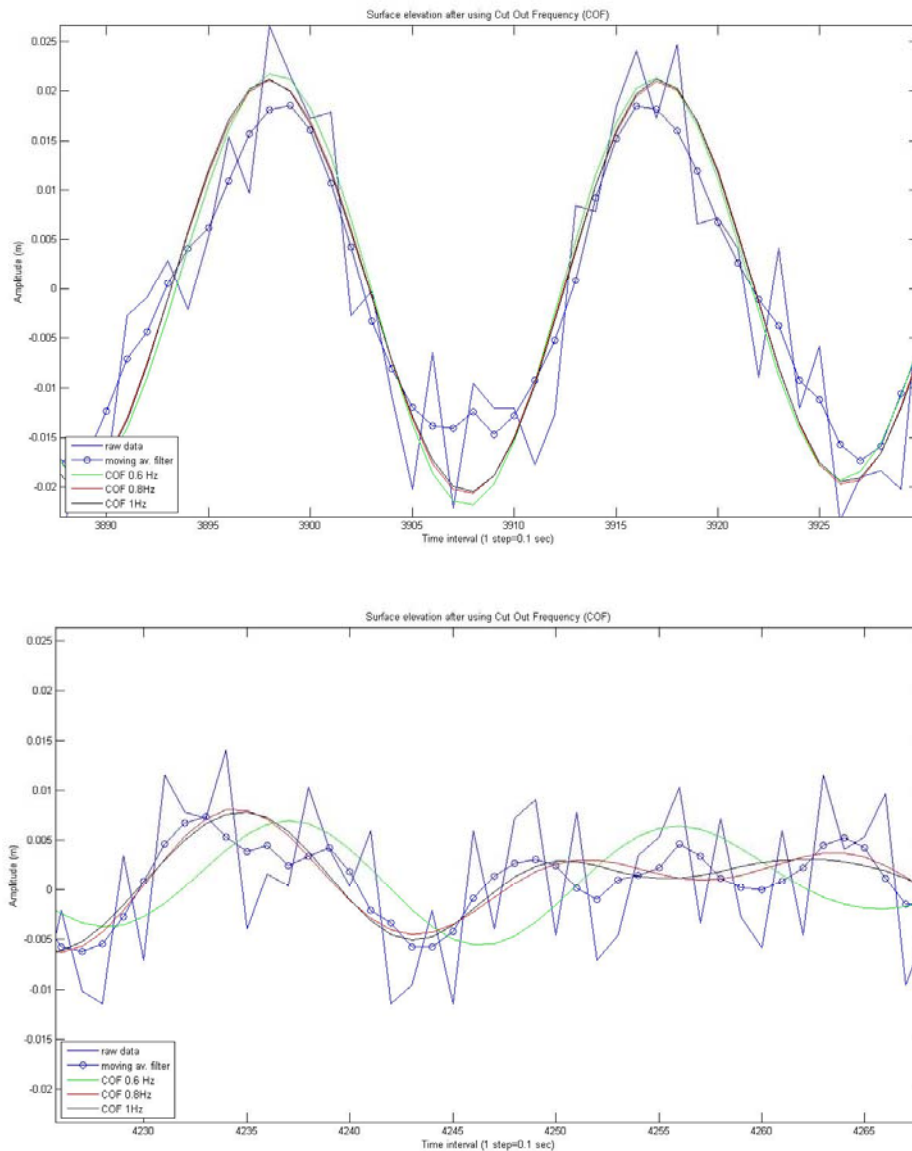
In any case, it is logical to think that using any COF frequency might remove some relevant component, resulting in the loss of validity of the process and data. Hence, the question is: up to which point the COF affects the validity data?

Below it is shown how the cut frequency affects the calculated the surface elevation for small/medium waves (30-30cm) and very small waves (about 10 cm).

Each figure shows 5 lines:

- The original time series gathered from the pressure sensor. Ripples and/or noise can be easily seen in the data (blue).
- A filtered time series of the raw data. That is calculated with a simple moving average filter, to try to show what the data would look like without noise (blue with circular markers).
- 3 time series (green, red and black lines) for which the above mentioned 3 COF have been used. These time series have been calculated starting from the raw data, using the FFT to divide it into frequency bins, using 1 of the 3 COF and then replicating the signal, once the high frequencies were removed.

As side note, if we were to analyze the raw data and replicate it without the use of any COF, the line would superimpose on the original time series.



It can be seen that for the small/medium waves (first case) the COF used has very small impact. The three lines (green, red and black) are very close together.

However, in the very small waves case (the second one), it can be seen that the green line (COF 0.6Hz) is separated from the other two (black and red). That represents the fact that, in absence of low frequency waves, the information removed by a lower COF is more visible. It has to be mentioned that the fact that the effect is more visible, doesn't necessarily mean that it is also relevant in the analysis.

### **Issues of using low and high COF**

To recap, the use of very low COF will corrupt the initial analysis of the raw data, removing relevant information from the time series.

However, the use of very high COF will corrupt the second part is the process (involved with  $K_p$ ), using frequencies that the pressure sensor is actually unable to capture. On this regard, having the pressure sensor as close as possible to the water surface would help.

## **Conclusion**

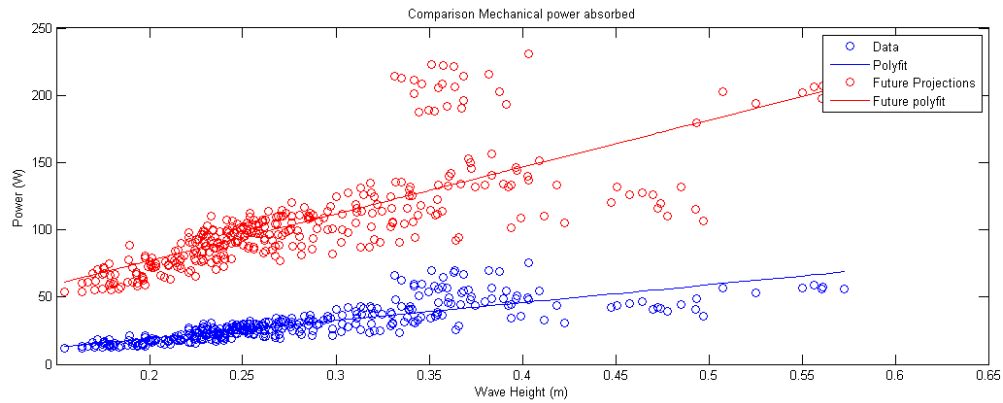
For this specific case, the best way to go to assure a correct analysis is the data is to take two corrections:

- Increase the COF from 0.6 to 0.8Hz (with damping factor of second order) to increase the accuracy of the first part of the process.
- Move the pressure sensor upward about 50 cm to increase the precision of the second part of the process.

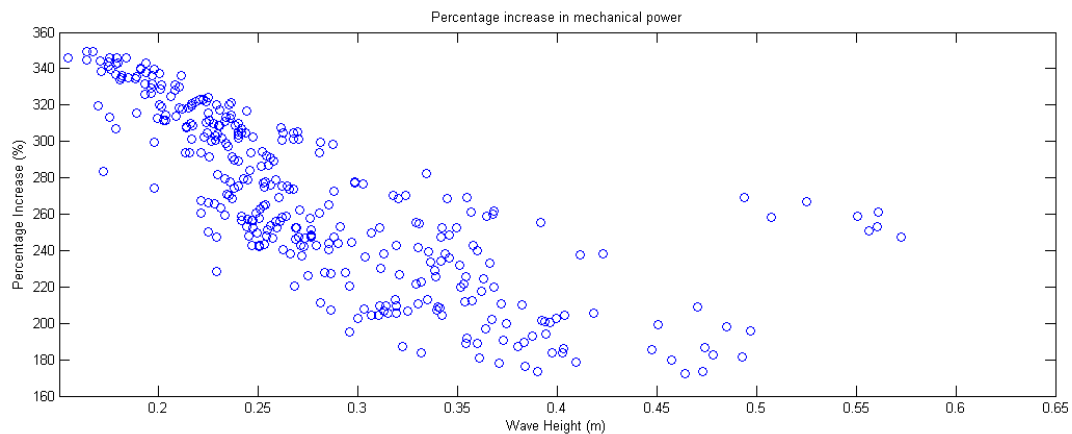
## APPENDIX C – Future improvements

With the data available it is possible to start making projections for future models that include different mechanical components.

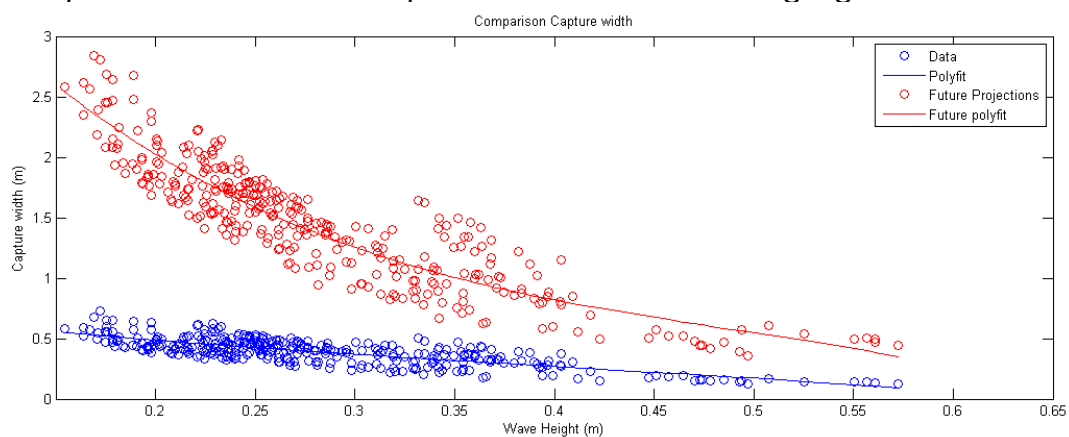
As an example, below it is shown how the device is expected to perform with the new and improved spring model currently in production, is introduced.



That would represent an increase in mechanical power as shown below:



Also the capture width would improve as in the following figure:



It has to be said that these are only calculated examples and will have to be checked and proved by real tests.

## **Recent publications in the DCE Technical Report Series**